ISSN: 2710-0588

Finite Element Analysis of Bond Behavior between Steel Plate, Prestressed CFRP, and Concrete

Mingdao Wang[1], Zhenjie Cui[1], Haoyu Cheng[1], Xueqian Xu[1]

[1]School of Civil Engineering, Liaoning University of Petrochemical Technology, Fushun 113000, China

Abstract

To investigate the interfacial bond behavior between steel plate-prestressed carbon fiber reinforced polymer (CFRP) sheets and concrete, a numerical model of the steel plate-prestressed CFRP sheet-concrete specimen was established via ABAQUS, and cohesive elements were adopted to simulate the nonlinear bond-slip characteristics of the interface. This study analyzed the influences of different prestress levels of CFRP sheets, bond lengths and CFRP sheet widths on the interfacial bond behavior between prestressed CFRP sheets and concrete in the single shear test model, as well as the bond-slip performance under the composite reinforcement of steel plates. The simulation results indicate that: compared with specimens without steel plates, the peak load of specimens with steel plates increases by approximately 16.8%, and the interfacial bond strength increases by 22.1%. Moreover, the post-peak load drops more gently, and the residual bearing capacity is higher. The prestress level has a significant effect on the interfacial bond behavior: when the prestress level increases from 10% to 20%, the interfacial peak stress and strength utilization rate increase significantly; when the prestress level reaches 30%, the peak stress decreases due to the accumulation of initial micro-damage. The effective bond length increases with the increase of prestress level. When the prestress level is excessively high and the bond length is insufficient, premature debonding occurs under interfacial loading. Under the condition that other parameters remain unchanged, when the bond length increases from 100 mm to 140 mm, the peak load increases by 16.3%, while the increase in bearing capacity is relatively marginal when the bond length is 180 mm, indicating that the effective bond length of CFRP sheets with 20% prestress is approximately 140 mm. When the width of CFRP sheet is 10 mm, tensile fracture occurs due to excessively small cross-sectional area; when the width is 20 mm or above, the failure mode transfers to interfacial debonding. Compared with bond length, increasing the width of CFRP sheet has a relatively limited effect on improving bearing capacity: when the width of CFRP sheet increases from 30 mm to 40 mm, the peak load of the specimen only increases by 5%. Based on the comprehensive analysis of various parameters, the optimal parameter combination is determined as 20% prestress level, 30 mm CFRP sheet width and 140 mm bond length. The numerical model proposed in this paper is verified by comparison with experimental results, and the research findings can provide a theoretical basis for the design and application of steel plate-CFRP composite reinforced concrete structures.

Keywords

Finite element analysis; Prestressed CFRP fabric; Bonding performance; Single shear specimen; Composite reinforcement.

1. Introduction

Carbon fiber reinforced composite fabric (CFRP fabric) has gained extensive attention and application in the field of concrete structure reinforcement due to its lightweight, high strength,

ISSN: 2710-0588

excellent corrosion resistance, and convenient construction. Compared with traditional methods such as increasing the section size and external steel application, the CFRP reinforcement technology has the significant advantages of almost no increase in structural self-weight, no change in structural appearance dimensions, and minimal damage to the original structure. It has become a research hotspot in the field of structural reinforcement [1-6]. When ordinary CFRP fabric is adhered for reinforcement, there is a serious stress lag phenomenon in the CFRP material, and its high strength performance often cannot be fully exerted [7-8]. In this context, the prestressed CFRP fabric reinforcement technology emerged. By applying prestress to the CFRP fabric, not only can the stress state of the reinforced component be improved, but the cracking load and yield load can also be effectively increased, and the strength utilization rate of the CFRP fabric can be significantly improved, thereby achieving a more ideal reinforcement effect [9-12].

With the promotion of the prestressed CFRP fabric reinforcement technology, the interface bonding and sliding behavior between CFRP fabric and concrete has become a key issue restricting the reinforcement effect. The interface is the only way to transfer loads between the CFRP fabric and concrete, and its bonding performance directly determines whether the high strength of the CFRP fabric can be fully exerted [13-15]. Domestic and foreign scholars have conducted a large number of studies on this issue. Wang Zhenzhen et al. [16] based on the cohesive force model, introduced a four-linear bonding sliding constitutive model with residual strength, simulated the interface peeling process between the CFRP plate and the concrete beam, and revealed the evolution laws of interface bonding shear stress, relative sliding amount, and the axial force distribution of the CFRP plate. Lu Huimin et al. [17-18] used the ABAQUS finite element software to simulate the bonding sliding relationship between the CFRP plate and concrete through nonlinear spring elements, and investigated the influence of prestress level, bonding length, and other factors on the bending performance of the reinforced beam.

Based on the existing research, the bonding performance of the CFRP fabric-concrete interface system or the CFRP fabric-steel plate interface system is usually the bonding performance of two-layer systems. Longlong Chen et al. [19] conducted numerical research on the prestressed unbonded CFRP plate reinforcement of steel-concrete composite beams, and found that the prestress level of the CFRP plate had a limited effect on the bearing capacity of the reinforced beam, but had a significant effect on its ductility, and pointed out that the ideal prestress level was 10% to 30%. However, research on the interface bonding sliding of the composite system of steel, CFRP fabric, and concrete is still relatively limited.

The bending performance of the composite reinforced beam is actually the result of the interaction of concrete compression, steel tension, and composite material tension, and is a relatively complex superimposed effect [20-25]. Any failure in any of these links will affect the failure mode of the beam. In practical situations, the interface bonding is usually relatively weak and prone to failure. Once the bonding interface is damaged, the reinforcement effect of the structure will be greatly reduced, and even lead to the failure of the structure. The bonding strength, effective bonding length, sliding amount, fracture energy, etc. will all affect whether the composite material can fully exert its function in the beam. Therefore, the bonding characteristics of the interface between steel-CFRP fabric-concrete are one of the key points in the mechanical properties of CFRP fabric and steel composite reinforced concrete structures. This paper takes the steel plate-CFRP fabric composite reinforcement of concrete as the research object. Using the ABAQUS finite element software, a detailed numerical model is established to study the influence laws of key parameters such as the degree of prestress, the width of the CFRP fabric, the bonding length, and the comparison of whether there is a steel plate or not on the interface bonding slip behavior. The failure mechanism and bonding-slip relationship of the CFRP fabric-concrete interface in this composite system are also studied,

ISSN: 2710-0588

providing a theoretical basis for the design and application of this type of composite reinforcement system.

2. Model specimen design

A total of three test specimens were designed for this experiment. The test method adopted was the "CFRP fabric - concrete lap joint method", and the loading method was single shear. Each specimen was formed by bonding two steel plates with a pre-stressed CFRP fabric to form a "whole" structure. The connection with the concrete was studied to investigate the bonding and sliding problems. The size of the pre-stressed steel plate was 200mm × 30mm, and the material was Q235 grade steel. The CFRP used was grade I carbon fiber fabric, with a length of 480mm, a thickness of 0.167mm, an ultimate tensile strength of 3500MPa, and an elastic modulus of 230Gpa. The concrete was a 100mm × 100mm × 300mm C30 strength concrete. As shown in Figure 1, the schematic diagram of the single shear specimen. The specific parameters of the materials are as shown in Table 1. The grouping of the specimens and their specific parameters are shown in Table 2.

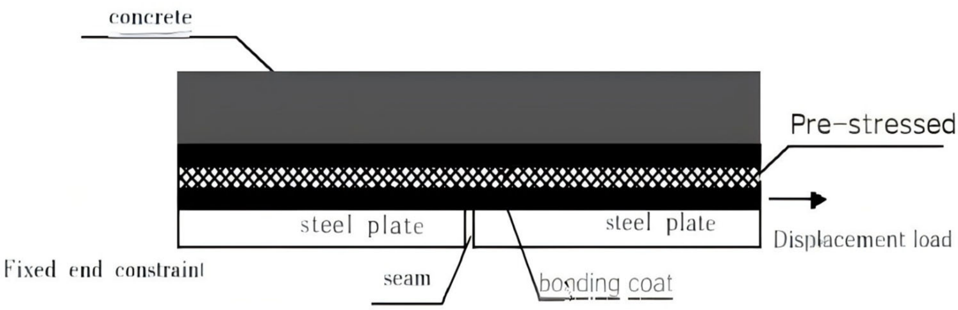

Figure 1. Schematic diagram of the single shear specimen

Table 1. Material Parameters

Material performance indicators	CFRP fabric	Impregnating glue	Q235 steel plate	concrete
Yield performance index / MPa	—	—	263	30
Tensile strength index / MPa	3597	40	—	2.01
Elastic modulus / MPa	2.46×105	2.5×103	2.01×105	3.50 × 103
maximum elongation	1.64	1.5	—	0.0033
Bending strength / MPa	—	50	—	4.5
Shear strength / MPa	—	20	—	2

Table 2. Finite Element Model Parameters

test-piece	The degree of prestressing in CFRP fabric	Width of CFRP fabric	Bonding length
BZ-1	20%	30mm	140mm
A-1	10%	40mm	140mm
A-2	30%	20mm	140mm
A-3	30%	30mm	140mm
B-1	20%	10mm	140mm
B-2	20%	20mm	140mm
C-1	20%	30mm	100mm
C-2	20%	40mm	180mm
BZ-2	20%	30mm	140mm

ISSN: 2710-0588

3. Finite Element Model

3.1. Model Assumptions

In order to facilitate the application of the established finite element model of CFRP fabric - bonding layer - steel plate in engineering, the following basic assumptions are made during the modeling process:

(1) Concrete, CFRP fabric and epoxy resin coating are all assumed to be continuous and uniform media.

(2) The CFRP fabric remains in a linear elastic working state throughout the loading process.

(3) The strains of concrete and the CFRP fabric itself are within the elastic range, but the geometric large deformation effect caused by interface peeling is considered.

(4) The interface between the CFRP fabric and the epoxy resin layer, and the interface between the epoxy resin layer and the concrete are ideal and completely bonded, with no relative sliding. All non-linear sliding behaviors are concentrated at the CFRP fabric - concrete contact interface or within the set adhesive layer elements.

(5) The loading rate is sufficiently slow, and inertial effects and dynamic influences are ignored. The problem is treated as a static one.

3.2. Material Constitutive Model

The constitutive relationship of the steel plate is set as a double-curve ideal elastic-plastic constitutive model, as shown in Figure 2. The analytical expression is as follows:

$$\begin{cases} E_{\varepsilon}, & \varepsilon \leq \varepsilon_y \\ f_y + E_1(\varepsilon - \varepsilon_y), & \varepsilon > \varepsilon_y \end{cases} \tag{1}$$

Here, f_y and ε_y represent the strength and strain values corresponding to the yield point of the steel, while fu and εu represent the ultimate strength and ultimate strain of the steel.

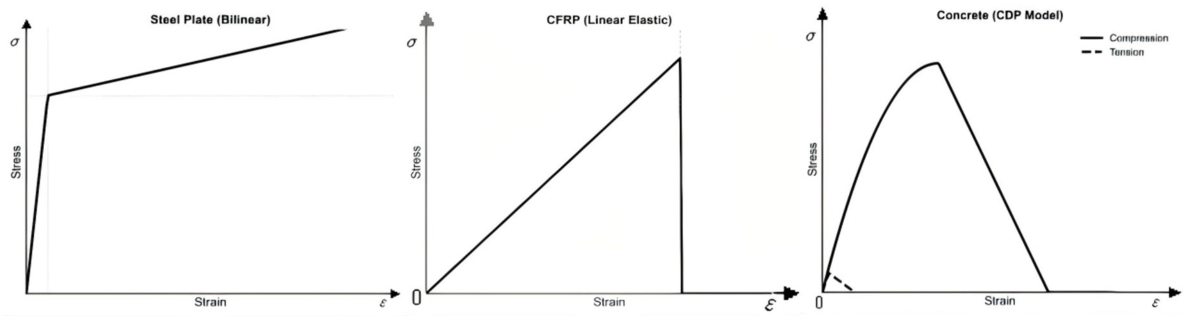

Figure 2. Steel, CFRP fabric, concrete - strain schematic diagram

This paper employs the traction-separation criterion cohesive element model to establish the cohesive-slip of the bonding layer as the simulation interface of the bonding layer, as shown in Figure 4. Here, τ_{max}, $\delta_{initial}$, and δ_{fail} represent the stress and displacement at the initial failure, and the displacement at complete failure. The damage criterion adopts the quadratic nominal stress criterion, and the basis for damage is:

$$\left\{\frac{\langle t_n \rangle}{t_n^0}\right\}^2 + \left\{\frac{t_s}{t_n^s}\right\}^2 + \left\{\frac{\langle t_t \rangle}{t_t^0}\right\}^2 = 1 \tag{2}$$

ISSN: 2710-0588

3.3. Establishment of the Finite Element Model

Based on the designed components and dimensions, using the finite element software ABAQUS and the separated modeling method, a pre-stressed CFRP fabric-concrete single shear specimen model was established, as shown in Figure 3. The concrete and steel plate were selected as the eight-node six-face element C3D8R; the CFRP fabric, due to its thickness of 0.167mm, was modeled using the 4-node curved shell element S4R to balance the calculation efficiency. Although in the actual specimen, the steel plate and the CFRP fabric were bonded through structural adhesive, this study mainly focused on the behavior of the external interface between concrete and CFRP fabric. The main function of the steel plate is to provide lateral restraint and additional stiffness to the CFRP fabric. To simplify the model and avoid introducing unnecessary complex parameters, the CFRP fabric and the steel plate surface were connected through a Tie. The grid of the pre-stressed CFRP fabric element was divided into 2.5mm, and the grid of the bonding layer element was divided into 1mm. Figure 4 shows the meshing of the single shear specimen model.

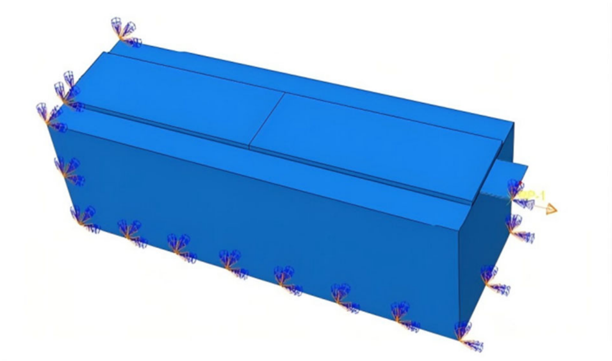

Figure 3. Single shear specimen model

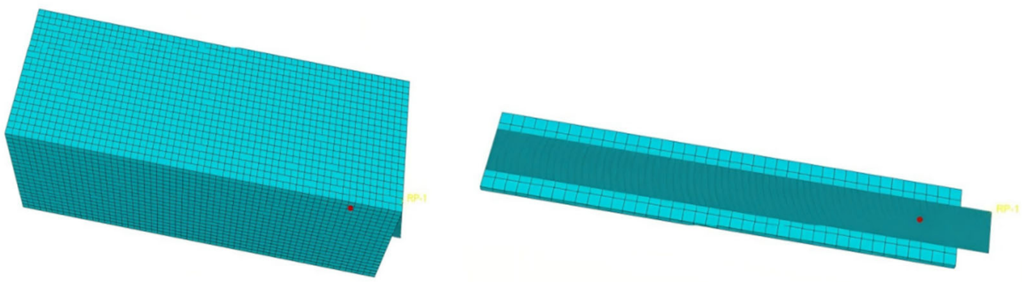

Figure 4. Material grid division

In ABAQUS, the "cohesive behavior" is employed and a bilinear traction-separation constitutive relationship is assigned to it. A zero-thickness cohesive element COH3D8 with zero thickness is created between the concrete surface and the neutral plane of the CFRP fabric to represent the adhesive layer and its failure process.

The model applies the cooling method [26] to apply prestress to the CFRP fabric. That is, through the predefined temperature field in the software ABAQUS, the temperature of the CFRP fabric is reduced, resulting in stress changes, which is used to simulate the actual test and pre-tension the CFRP fabric in advance to provide prestress. The temperature is calculated by the following formula [27]:

$$\Delta T=\frac{\sigma}{\alpha E} \tag{3}$$

ISSN: 2710-0588

4. Model Validation

4.1. Load Displacement Curve

To verify the correctness of this model, this paper adopts the numerical simulation study on the influence of FRP plate width on the concrete interface bonding performance by He Zhujie et al. [22], and combines it with the comparison results of the single shear specimens of steel plate-prestressed CFRP fabric and concrete from our research group to validate the correctness of the model.

The comparison table of the actual test limit load and limit displacement values of the specimens with the finite element simulation values is shown in Table 3. The load-displacement curves of the specimens BZ-1 and BZ-2 during the test and the finite element simulation are presented in Figure 7. From Figure 5 and Table 3, it can be seen that the test and model curves have a basically consistent trend. The simulated values have certain errors compared to the test values, but the errors are within a reasonable range.

In conclusion, the finite element model established in this paper is accurate and reasonable. Based on this model, the simulation calculation of the interface bonding performance between prestressed CFRP and steel can be conducted. In conclusion, the finite element model established in this paper is highly accurate.

Table 3. Model Validation

test-piece	Ultimate load (kN)	Limit displacement (mm)
Simulate 20% prestress	24.703	1.119
prestress test 20% prestress	25.224	1.154
Simulation without steel plates	18.53	7.258
Test with steel plates	20.153	7.263

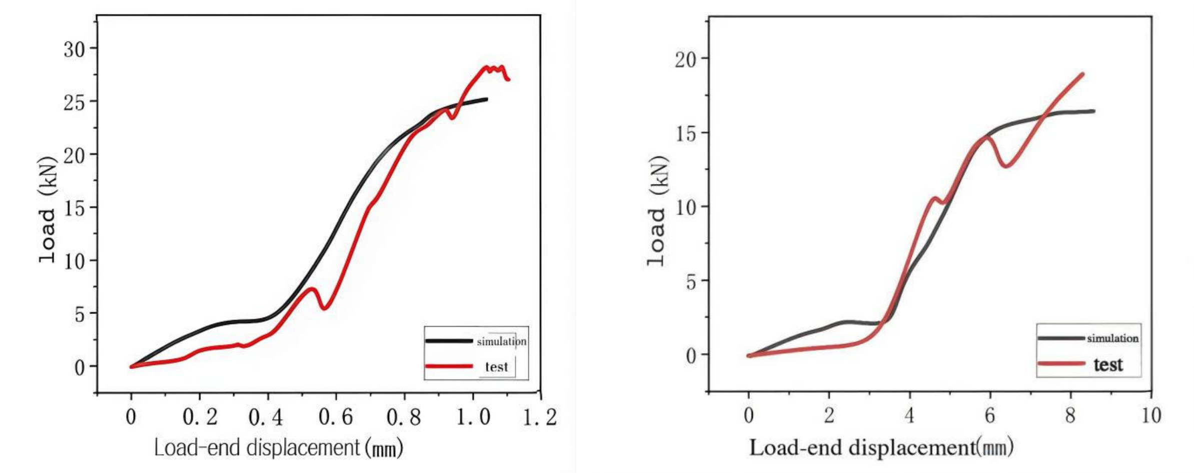

(a) Sample BZ-1 (a) Sample BZ-2

Figure 5. Load - Displacement Curve at Loading End

5. Result Analysis

5.1. Destruction Features and Destruction Patterns

5.1.1. The destruction process of CFRP fabric

Figures 6-a to 6-e show the stress diagrams of the CFRP fabric along the length direction corresponding to BZ-1. From the figures, it can be seen that during the stretching process, the

ISSN: 2710-0588

CFRP fabric with the steel plate part is subjected to more uniform force, and has stronger bonding performance and ductility. As the failure process progresses, the area with stress on the CFRP fabric gradually extends towards the fixed end. During the process of the load increasing from 0 Pu to 1.0 Pu, the range of stress variation gradually increases, indicating that after the bonding interface begins to peel off until the ultimate load, its effective bonding length gradually increases rather than remaining constant. From the elastic stage to the specimen failure, the color of the CFRP fabric cloud diagram at the initial bonding position changes from light blue → green → yellow → orange → red, indicating the state that the strain of the CFRP fabric gradually increases during the loading process.

(a) Test specimen BZ-1 cloud image

(b) Test specimen BZ-1 cloud image

(c) Test specimen BZ-1 cloud image

(d) Test specimen BZ-1 cloud image

(e) Test specimen BZ-1 cloud image

Figure 6. Stress Map of Carbon Fiber Cloth

5.1.2. The destruction process of epoxy resin adhesive

Based on the visual analysis results obtained from ABAQUS, it can be observed that the damaged area of the adhesive layer gradually expands, but it does not extend to the fixed end. Instead, it stops developing at a certain distance from the fixed end, as shown in Figures 7-a to 7-d. This indicates that the length of the bonding segment after this position is shorter than the effective bonding length, and it is unable to continue bearing a higher load, thus causing the overall load to decrease at this point. From the damage cloud map, it can also be observed that the damage of the adhesive layer always shows a distribution feature of heavy at the edges and light in the center, and when it finally fails, the edge area of the adhesive layer is the first to completely fail.

ISSN: 2710-0588

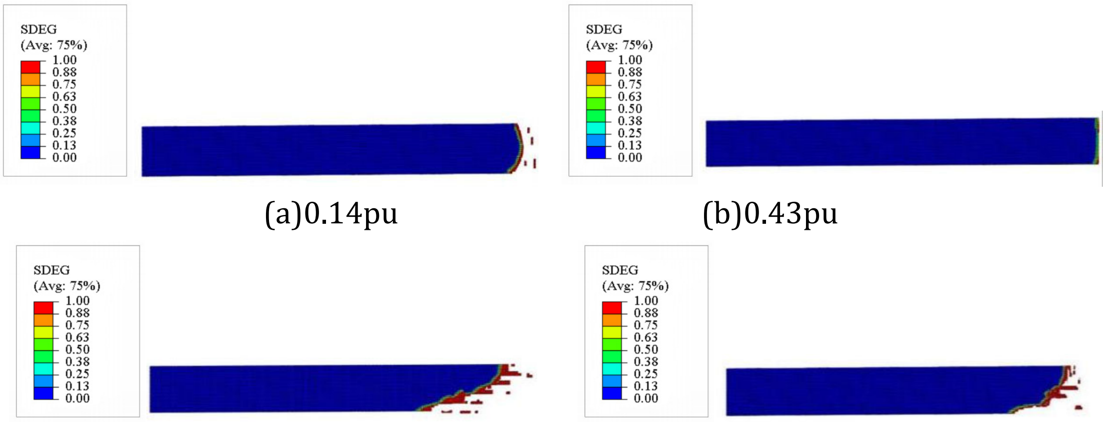

(a)0.14pu (b)0.43pu

(c)0.77pu (d)1.0pu

Figure 7. Failure process of epoxy resin adhesive in the finite element model

From the figure, it can be seen that as the damage process progresses, there are not many changes at the end of the adhesive layer. This indicates that although the shear force continues to be transmitted downward after reaching the effective bonding length, the bonding force no longer increases. This result suggests that as the bonding length increases, the utilization rate of the CFRP fabric and the concrete bonding surface is decreasing. After exceeding the effective bonding length, even if the bonding length increases, the ultimate bonding force will not increase.

Tables 4 to 6 show the variation of the peak stress of the CFRP fabric when the specimen fails under different parameters. Table 3 indicates that as the prestress increases from 10% to 20%, the peak stress at the time of CFRP fabric failure significantly increases. When the prestress level further increases to 30%, the peak stress shows a downward trend, presenting a pattern of first increasing and then decreasing. Table 5 shows that by increasing the bonding length of the CFRP fabric in the specimen, the peak stress changes for 140mm and 180mm are relatively small. Table 5 explains that by changing the width of the CFRP fabric, the fluctuation of the peak stress changes for CFRP fabrics with widths of 20mm, 30mm, and 40mm is relatively small.

Table 4. Peak Stress Changes of CFRP Sheets in Prestress Degree Groups

test-piece	Degree of prestress	Gel layer length (mm)	Width of CFRP fabric (mm)	The peak stress variation range of CFCFRP fabric
A-1	10%	140	40	5.4%
BZ-1	20%	140	30	——
A-2	30%	180	20	-1.6%
A-3	30%	140	30	3.6%

Table 5. Peak stress variation of CFRP fabric in the bonding length group

test-piece	Degree of prestress	Gel layer length (mm)	Width of CFRP fabric (mm)	The peak stress variation range of CFCFRP fabric
C-1	20%	100	30	0.5%
BZ-1	20%	140	30	——
C-2	20%	180	40	2.3%

ISSN: 2710-0588

Table 6. Changes in peak stress of CFRP fabric width groups

test-piece	Degree of prestress	Gel layer length (mm)	Width of CFRP fabric (mm)	The peak stress variation range of CFCFRP fabric
B-1	20%	100	20	-0.24%
BZ-1	20%	140	30	——
B-2	20%	180	40	5%

5.2. Load - Displacement Curve at Loading End

As shown in Figure 8(a), there were significant differences in the load-displacement curves of the specimens in different prestress levels groups. The CFRP fabric in this group had different degrees of prestress, and thus the bonding force formed with the bonding layer was also different. At a prestress level of 10% and 20%, the curves showed a linear and steady upward trend. However, the ultimate load and ultimate displacement that the 30% prestressed fabric could withstand were lower than those of the BZ-1 fabric with a 20% prestress level. This was because as the prestress increased, the distribution of the bonding shear stress at the CFRP-cement interface became more uniform, effectively alleviating the stress concentration at the loading end, and delaying the initiation and expansion of the separation. However, when the prestress was too high, the accumulation of micro-damage at the interface or the intensification of stress concentration at the end weakened its inhibitory effect on interface separation, causing the CFRP fabric to fail at a lower stress level [6].

As shown in Figure 8(b), the load-displacement curves of the specimens with different bonding lengths all went through three stages: initial non-linear adjustment, linear growth, and subsequent peak load and loading-end displacement drop. When the bonding length was 100mm, the peak load of the specimens was lower, and the curve showed a shorter linear growth segment, with the load rapidly decreasing after reaching the peak, presenting a brittle separation failure characteristic. This is because the 100mm bonding length had not reached the effective bonding length of the CFRP-cement interface, and the stress transfer area was insufficient to fully utilize the strength of the CFRP fabric, causing the interface to separate at a lower load.

As shown in Figure 8(c), this group of specimens had the same prestress and bonding length, with the width of 30mm and 40mm materials having relatively small performance changes, all experiencing separation failure. However, the 20mm-width CFRP fabric, when pre-stressed with a large force in advance, was broken by the tensile force.

5.3. Comparison of Steel Plate Parameters

To investigate the role of the steel plate in the CFRP fabric-concrete composite reinforcement system, this section compares the mechanical response differences between the steel plate test specimen BZ-1 and the steel-free test specimen BZ-2. Figure 9 shows the load-displacement curve of the steel plate group.

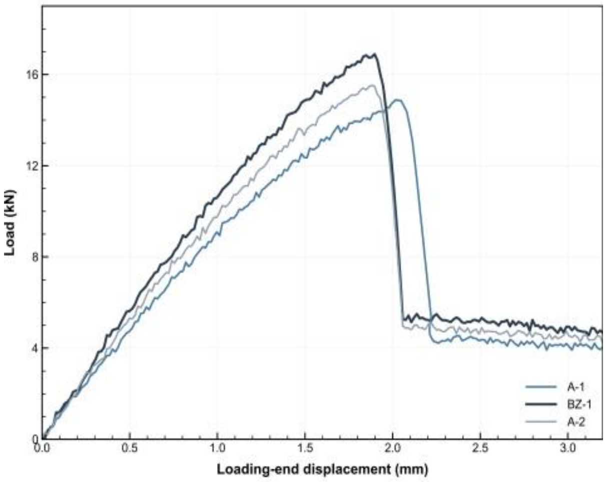

(a) Prestress level group

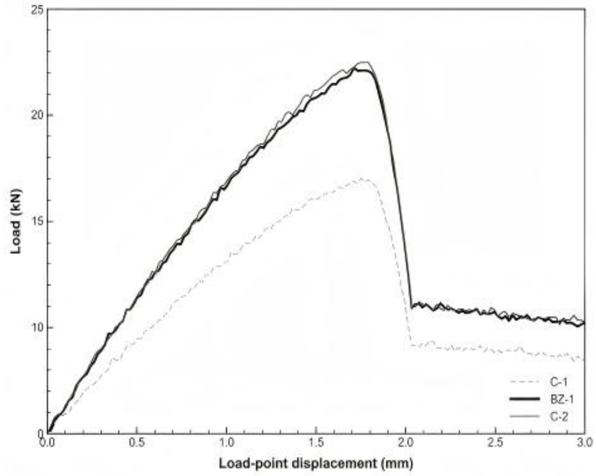

(b) Bonding Length Group

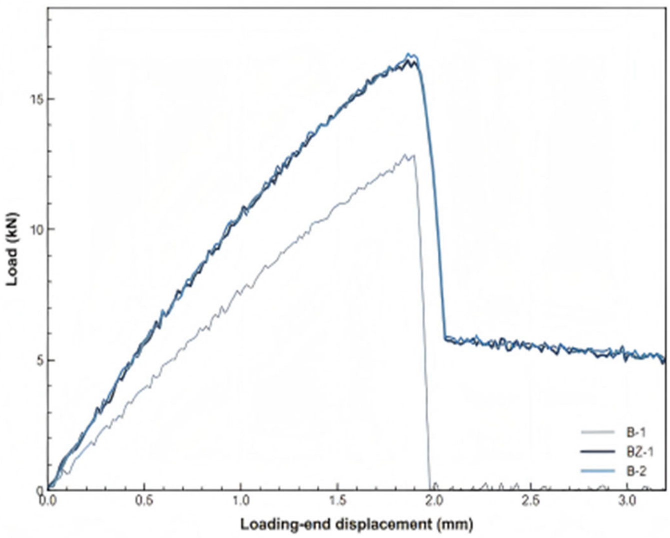

(c) CFRP fabric width group

Figure 8. Load-end Displacement Curve

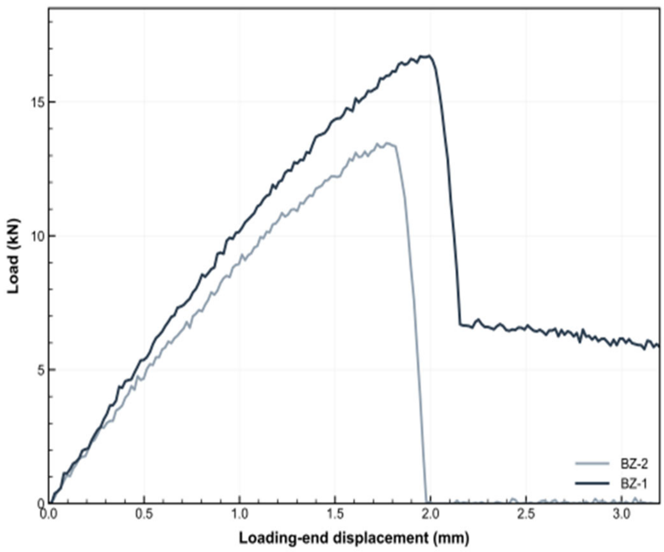

Figure 9. Load-displacement curve of the steel plate group at the loading end

ISSN: 2710-0588

From the figure, it can be observed that the slope of the curve for the steel plate specimens is greater, indicating that the presence of the steel plate significantly enhances the overall stiffness of the specimen in the elastic stage. In terms of ductility, the load drop curve after the peak value for the specimens with steel plates is more gentle, demonstrating better deformation capacity. For the specimens without steel plates, almost all the bearing capacity is lost after the CFRP fabric-cement bond separation; while for the specimens with steel plates, after the bond separation, the steel plates bear most of the load, thus forming a stable residual bearing capacity stage, improving the peak bearing capacity of the specimen and also enhancing its ductility. It can effectively delay the bond separation in the continuous CFRP bond separation stage. Some literature conducted four sets of self-anchored in-plane double shear tests, dividing the process of CFRP fabric-mixed carbon fiber fabric from initial loading to failure into three stages. The study shows that the steel plate anchor can delay the bond separation of the carbon fiber fabric, increasing the interface bonding strength by 18.02%[15]. The peak load in the steel plate condition is approximately 16.8 kN, while the peak load in the non-steel plate condition is approximately 13.5 kN, which is an increase of about 22.1%. This improvement is consistent with the conclusion in the literature that composite reinforcement can significantly enhance the bearing capacity of the component.

5.4. Interface shear stress distribution

Through analysis, the shear stress at the interface between the prestressed CFRP fabric and concrete for each specimen under the same frame rate was extracted. Figure 10 shows the visual distribution map of the shear stress at the concrete interface during the loading process of specimen BZ-1. Figure 11 shows the distribution curves of the interface shear stress for each specimen. From Figures 9 and 10, it can be seen: ① In the initial loading stage, the interface is in the elastic stress transfer stage. The tensile force of the CFRP fabric gradually transfers from the loading end to the free end, and the shear stress distribution at the interface shows a high value at the loading end and a low value at the free end.② The influence of the magnitude of prestress on the shear stress distribution at the interface is relatively small. By comparing the shear stress distribution curves of specimens A-1, BZ-1, and A-3, the trend of the shear stress distribution of the three specimens is relatively close, and the distribution law of shear stress on the specimen interface has not changed significantly.③ There is an effective bonding length at the interface. When the effective bonding length is reached, the shear stress at the interface is almost zero. By comparing the shear stress distribution curves of the prestressed CFRP fabric of group A specimens, the effective bonding length of the specimens in group A remains at around 100mm. From specimen BZ-1 and group B specimens, it can be known that the effective bonding length of the specimens increases with the increase of the width of the CFRP fabric. And the narrower the width, the less uniform the shear stress distribution. A wider CFRP can make the adhesive area more effectively disperse and transfer the shear force, reducing the phenomenon of stress concentration. By comparing specimen BZ-1 and group C specimens, the influence of the effective bonding length on the shear stress distribution of the specimen is small.

④ By comparing specimens with and without steel plates ZB-1 and ZB-2, it can be found that the interface of the specimen without steel plates is because there is only the bonding layer to resist the shear stress. When the load reaches a certain level, the bonding force is damaged, and the shear stress distribution rapidly deteriorates, the load drops sharply, and the brittle characteristic is obvious. While the presence of steel plates can delay the failure of the specimen. The shear stress can still maintain a stable distribution after reaching the peak value.

ISSN: 2710-0588

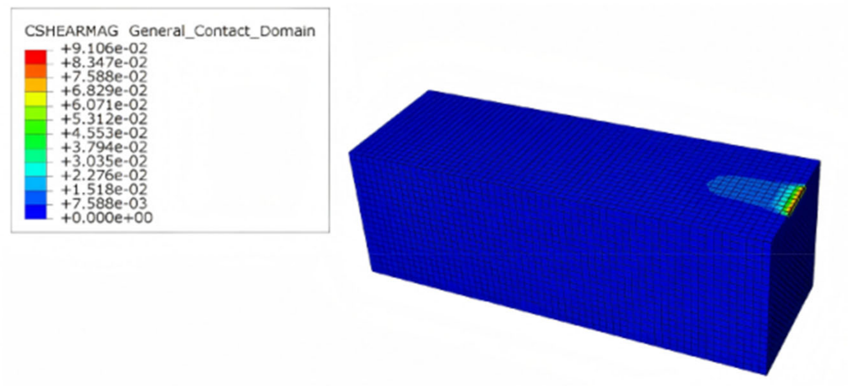

10(a) Visual diagram of concrete stress

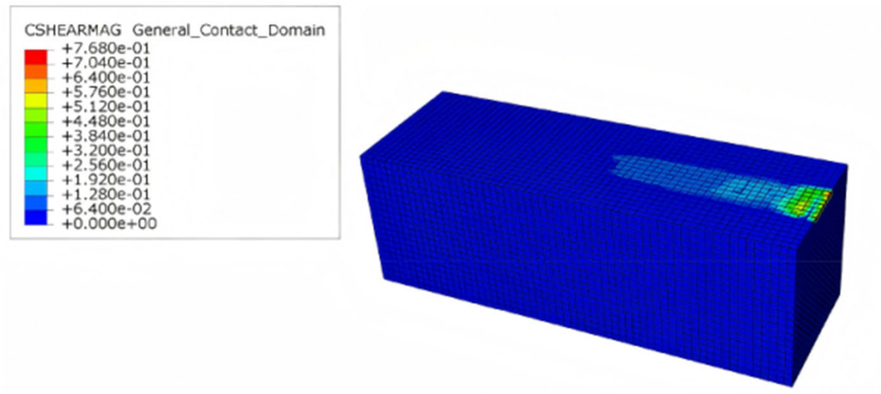

10(b) Visual diagram of concrete stress

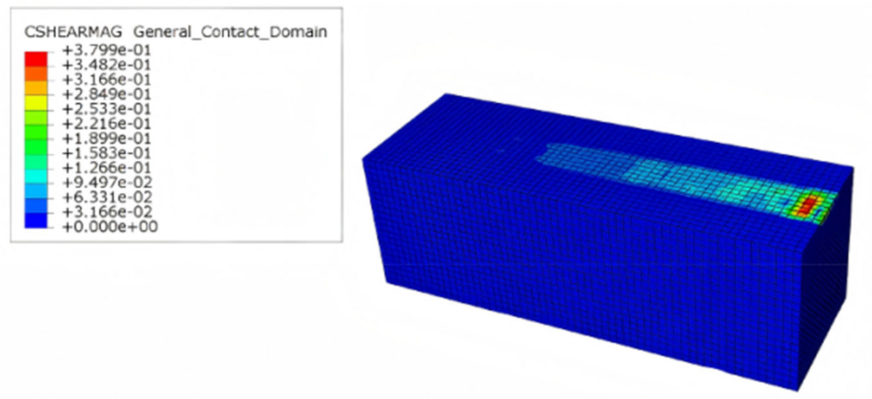

10(c) Visual diagram of concrete stress

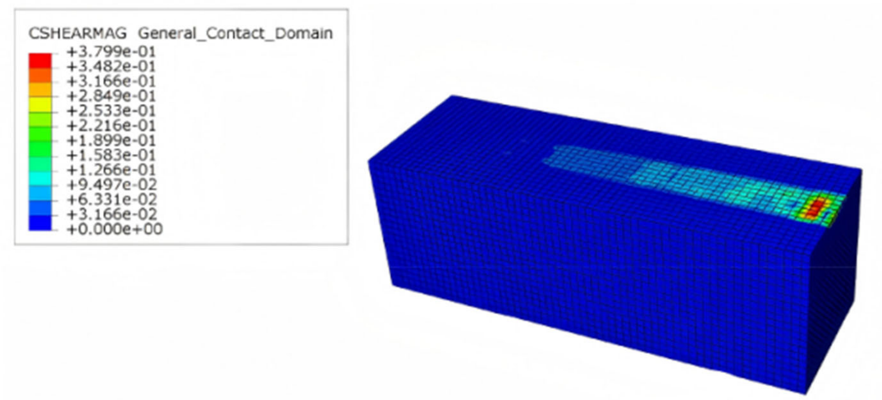

10(d) Visual diagram of concrete stress

Figure 10. Cloud chart of concrete stress variation

ISSN: 2710-0588

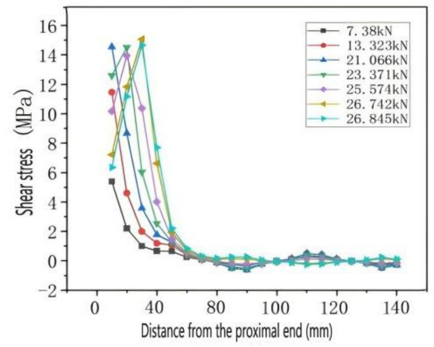

(a) A-1

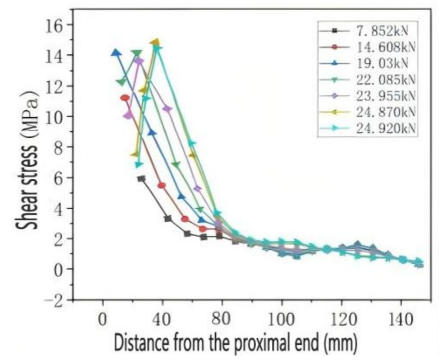

(b) A-2

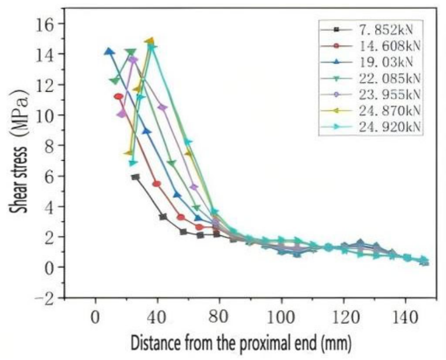

(c) A-3

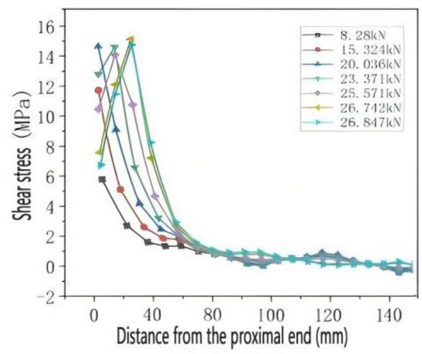

(d) ZB-1

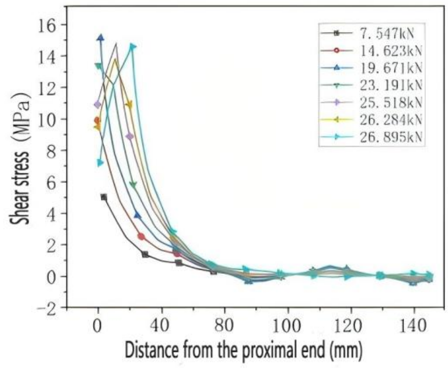

(e) B-1

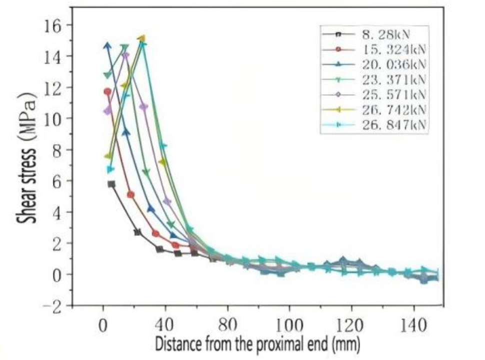

(f) B-2

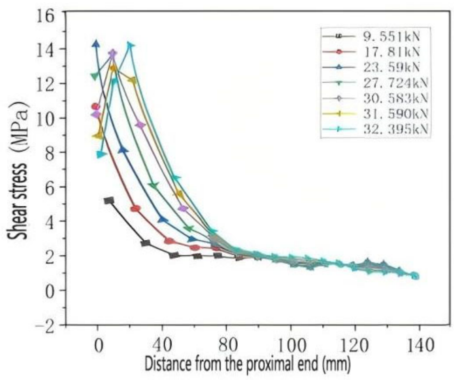

(g) c-1

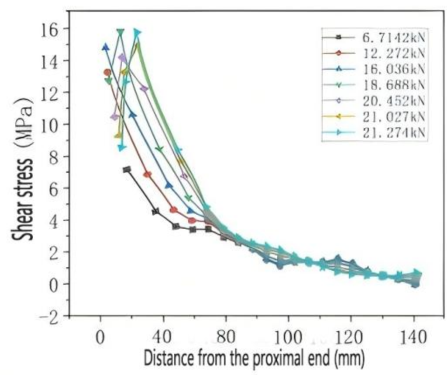

(h) c-2

Figure 11. Bonding Slip Curve Graph

ISSN: 2710-0588

5.5. Bonding Slip Relationship

The bond-slip relationship (τ-δ curve) describes the intrinsic mechanical relationship between the local bond stress τ and the slip amount δ at the interface between CFRP fabric and concreteFor each group of specimens, the shear stress and displacement relationship of the interface bond layer were extracted, and the bond-slip curves for each group of specimens were plotted. Based on the bond-slip constitutive relationship of FRP-concrete interface proposed by Lu Xinzheng et al. [20], a bilinear model suitable for analytical analysis was selected to characterize the mechanical behavior of the CFRP fabric-concrete interface. This model can be expressed by the following equation:

$$\tau=\tau_{max}\cdot\frac{\delta}{\delta_0}(0\leq\delta\leq\delta_0) \tag{4}$$

$$\tau=\tau_{max}\cdot\frac{\delta_f-\delta}{\delta_f-\delta_0}(0\leq\delta\leq\delta_0) \tag{5}$$

Among them, τmax represents the interface bonding strength (MPa); δ0 is the peak slip amount (mm); δf is the ultimate slip amount (mm). The interface failure energy Gf (N/mm) is equal to the area under the τδ curve, and the formula is:

$$G_f=\int_0^{\delta_f}\tau(\delta)d\delta=\frac{1}{2}\tau_{max}\,\delta_f \tag{6}$$

In this study, as mentioned above, the effective bonding length between the CFRP fabric and concrete is approximately 140mm. Therefore, the key parameters of the τ-δ curve selected are as follows:

$$\tau^{max} = 6.0\text{ Mpa};\ \delta_0 = 0.15\text{ mm};\ \delta_f = 0.50\text{ mm}$$

The curve shows that when the interface displacement δ is less than 0.15 mm, the bonding stress τ increases nearly linearly with the increase in displacement, and the interface is in the elastic stage. When the displacement reaches 0.15 mm, the bonding stress reaches its maximum value τmax, which is the interface bonding strength. At this point, initial peeling begins to occur at the interface. When the displacement exceeds 0.15 mm, the bonding stress enters the descending segment. As the displacement continues to increase, the interface peeling damage accumulates continuously, and the residual bonding capacity gradually decreases. The morphology and development pattern of the entire bonding displacement curve describe the entire process of the CFRP-concrete interface from elastic operation, to damage evolution, to final peeling failure, which is consistent with the report in the literature. Figure 12 is the bonding-displacement curve diagram of specimen BZ-1. Gf represents the strength of the interface's energy absorption ability during the peeling failure process. The higher the value, the more energy is required to consume during the process from the emergence of the interface crack to its complete failure, that is, the stronger the interface's ability to resist peeling failure.

ISSN: 2710-0588

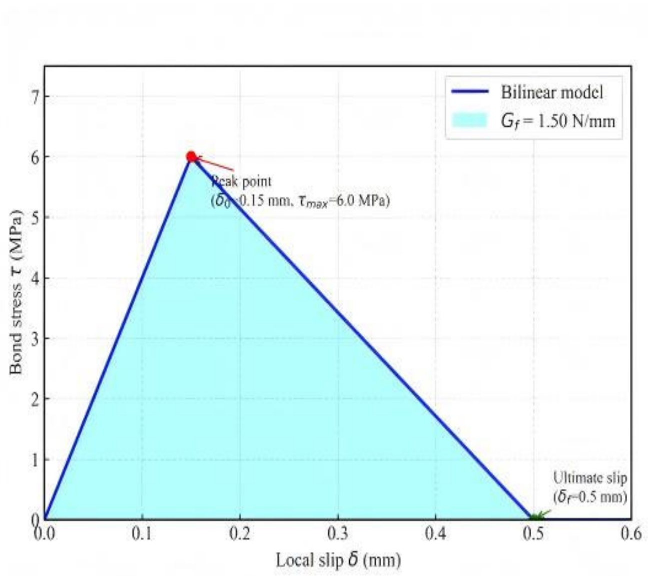

Figure 12. Bilinear Bonding Slip Relationship

Figure 13 shows the bond-slip curves at different positions along specimen BZ-1 from the near end. It can be observed that the bond-slip curves at various locations do not coincide; however, those at positions between 0 and 15 mm exhibit similar trends, all undergoing a complete process of shear stress wave propagation. Beyond 15 mm, the bond-slip curves gradually become flatter, indicating that as the distance from the near end increases, both the applied shear stress and resulting slip decrease. This further confirms the conclusion in Section 5.3 of this paper that when reaching the critical position corresponding to the effective bond length, the interfacial shear stress is nearly zero. However, in theoretical analysis, it is assumed that the stress distribution across the cross-section of the CFRP sheet remains uniform during the elastic stage, and thus the changes occurring at each point within the bonding layer are also uniform. For reference analysis in this experiment, the bond-slip curve at the position 40 mm from the near end was selected, as this point experienced a complete shear stress wave transmission process.

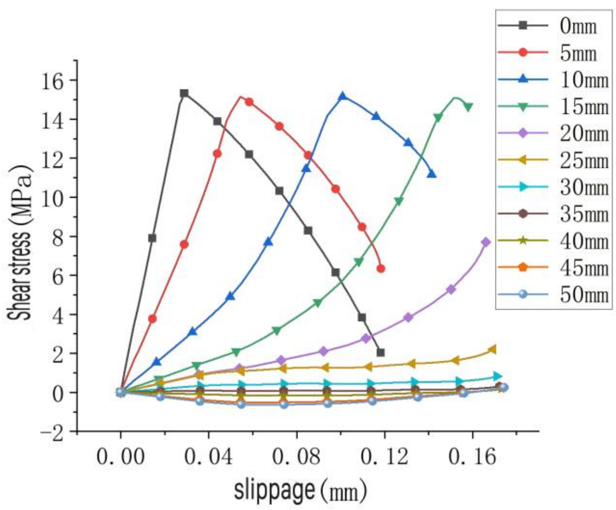

Figure 13. Bond-slip curves at different positions of specimen BZ-1

Figure 14 shows the bond-slip curves at a position 40mm proximal to the end for three groups of specimens. By combining these three figures, it can be observed that the bond-slip curve of the interface can be divided into two stages - the ascending stage and the descending stage. The three short vertical lines in the figure (red, black, and blue) are used to distinguish the ascending and descending stages of each specimen. During the initial loading of the specimens, the interface shear stress and relative slip show a linear growth relationship, indicating that the interface has good linear elasticity. As the load continues to increase, the stiffness of the interface begins to decrease, the slope of the bond-slip curve begins to decrease until it becomes 0, and the interface bonding layer enters the damage stage, and the curve begins to enter the descending stage. In the descending stage, as the load increases, the deterioration rate of the interface performance accelerates until the prestressed CFRP fabric and the concrete interface peel off, and the cohesive failure of the bonding layer occurs.

As can be seen from Figure 14(a): Different levels of prestress are the key parameters affecting the constitutive relationship of the bond-slip at the CFRP-cement interface. The shear test with the initial prestress of CFRP as the influencing factor shows that the relationship curves between the interface bonding stress and the slip amount under different prestress levels have significant differences. When the prestress increases from 10% to 20%, the peak shear stress τ_{max} of the τ-δ curve significantly increases, the descending section becomes more gentle, and the interface ductility improves; when the prestress is further increased to 30%, the peak stress of the curve decreases instead.

As can be seen from Figure 14(b): when the bonding length is 100mm, the effective bonding length has not been reached, and the τ-δ curve is incomplete, with a relatively low τ_{max}; when the bonding length reaches 140mm, the τ-δ curve shows a complete ascending and descending segment, and τmax reaches a relatively high level; when the bonding length increases to 180mm, τmax no longer significantly increases, but the descending segment becomes more gentle. The research on the end anchorage of CFRP fabric-concrete interface also indicates that different bonding lengths have a significant impact on the force behavior of the interface throughout the process[30].

As can be seen from Figure 14(c): The influence of different CFRP fabric widths. When the width is only 10mm, the shear stress is concentrated near the loading end, the interface stress transfer efficiency is low, and the τ-δ curve is truncated at a smaller slip amount, and the failure mode is CFRP bristle fracture. When the width increases to 30mm, the distribution of shear stress along the width direction becomes more uniform, the edge stress concentration is alleviated, the interface stress transfer efficiency is improved, and the τ-δ curve presents a complete ascending and descending segment shape. The prestress parameters are the same, but when the width is 10mm, due to the small cross-sectional area of the CFRP fabric, the failure mode changes to CFRP bristle fracture, and the τ-δ curve cannot completely describe the interface peeling process and breaks. However, when the width of the CFRP fabric reaches 40mm, the effect is only slightly better than that of the 30mm width. Therefore, in this study, the combination of 20% prestress, 30mm width, and 140mm bonding length makes the τ-δ curve show a better effect.

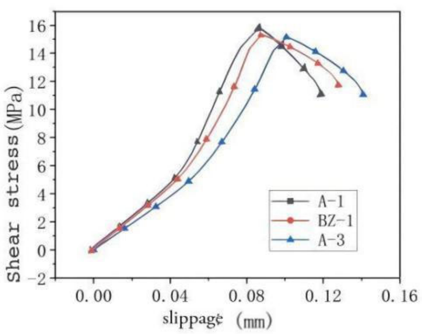

Figure 14-a. Prestressed group

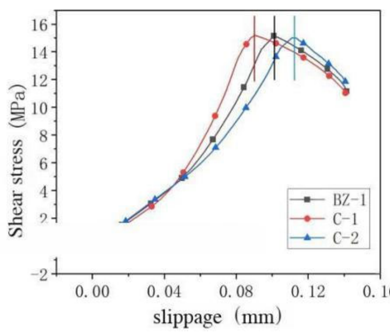

Figure 14-b. Bonding length group

ISSN: 2710-0588

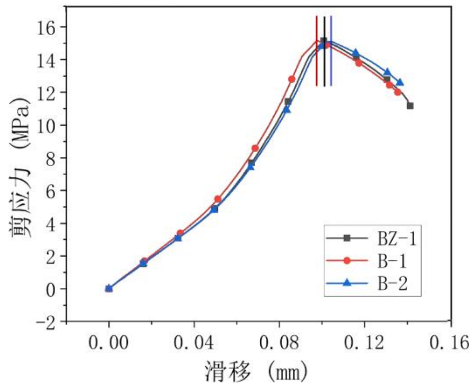

Figure 14-c. CFRP fabric width group

6. Conclusion

A model of steel plate - prestressed CFRP fabric and concrete single shear specimen was established using the finite element software ABAQUS. With the prestress degree of the CFRP fabric, the bonding length and the width of the CFRP fabric as parameters, the performance of the interface was investigated and the following conclusions were drawn:

(1) The cohesive failure within the bonding layer is the main failure mode of the prestressed CFRP fabric-concrete single shear specimens; at this time, the peak stress of some prestressed CFRP fabric has not yet reached the limit state.

(2) When the prestress level increases from 10% to 20%, the distribution of bonding shear stress at the CFRP fabric-concrete interface becomes more uniform, the stress concentration at the loading end is effectively alleviated, the interface peeling is significantly postponed, and the peak stress and strength utilization rate of the CFRP fabric have both been significantly improved. When the prestress level further increases to 30%, excessive prestress leads to an intensified stress concentration at the end, weakening the inhibitory effect of prestress on peeling, and the peak stress of the CFRP fabric actually decreases compared to 20%. Based on the analysis of the load-displacement curve, 20% prestress is the optimal prestress level in this composite reinforcement system.

(3) When the width of the CFRP fabric is 10mm, due to the small cross-sectional area, its own tensile bearing capacity is lower than the interface bonding bearing capacity. The failure mode is that the CFRP fabric is pulled apart, and the τ - δ curve is truncated at a slip distance of approximately 0.25mm. When the width increases to 20mm, the failure mode changes to interface peeling; at 30mm width, the interface bonding performance is fully exerted, and the τ-δ curve presents a complete ascending and descending segment; further increasing to 40mm, the bearing capacity gain is limited. In this study, 30mm is the optimal width of the CFRP fabric.

References

[1] Mei, K. H., Wang, F. X., & Sun, S. J. (2024). Research progress on fiber-reinforced composite materials for strengthening concrete bridge structures. *Journal of Architectural Science and Engineering*, (01), 31–51. https://doi.org/10.19815/j.jace.2022.09044.

[2] Lu, Y. Y. (2018). Research progress on composite reinforcement of concrete structures using fiber-reinforced composites and steel. *Journal of Building Structures*, 10, 138–146. https://doi.org/10.14006/j.jzjgxb.2018.10.016

[3] Pang, Y., Wu, G., Wang, H., Gao, D., & Zhang, P. (2021). Bond-slip model of the CFRP-steel interface with the CFRP delamination failure. *Composite Structures*, 256, 113015. https://doi.org/10.1016/j.compstruct.2021.113015

[4] Wang, X. L., Li, C. F., & Li, K. (2019). Experimental analysis of bond performance of CFRP-reinforced damaged reinforced concrete beams under fatigue loading. *Building Structure*, (03), 87–91. https://doi.org/10.19701/j.jzjg.2019.03.016

[5] Zhang, L. (2020). Experimental and theoretical analysis on the bonding performance of CFRP-solid interface under static load and fatigue load [Doctoral dissertation]. Southeast University. https://doi.org/10.27014/d.cnki.gdnau.2020.000066

[6] Zhu, G. S., Zhu, F. S., Sheng, G. H., & Ma, Z. X. (2018). Analysis of bending load, stiffness and cracks of T-shaped beams strengthened with prestressed CFRP and steel plates. *Journal of Shenyang Jianzhu University (Natural Science Edition)*, (02), 211–221.

[7] Ding, J. S., Niu, P., Wang, X. C., Jin, C. F., & Guo, Q. (2020). Research progress on prestressed CFRP plate reinforcement of concrete bridges. *Concrete*, (09), 133–138.

[8] Lü, Z. H., Xu, H. B., & Yu, Q. Q. (2022). A review of CFRP-solid bonding performance under fatigue loading. *Structural Engineers*, (05), 177–181. https://doi.org/10.15935/j.cnki.jggcs.2022.05.011

[9] Hu, L. L. (2020). Research on the overall stability of steel columns reinforced with prestressed carbon fiber composite plates [Doctoral dissertation]. Tsinghua University. https://doi.org/10.27266/d.cnki.gqhau.2020.000045

[10] Ye, H. W. (2009). Experimental study on the tensile static and fatigue properties of prestressed carbon fiber reinforced plate (CFRP) strengthened steel plates [Doctoral dissertation]. Southwest Jiaotong University.

[11] Zhu, G. S., Zhu, F. S., & Sheng, G. H. (2018). Experimental study on the bending resistance of T-beams strengthened with prestressed CFRP and steel plate composites. *Journal of Northeastern University (Natural Science Edition)*, (04), 594–598.

[12] Lu, X. Z., Ye, L. P., Teng, J. G., & Jiang, J. J. (2005). Meso-scale finite element model for FRP sheets/plates bonded to concrete. *Engineering Structures*, 27(4), 564–575. https://doi.org/10.1016/j.engstruct.2004.10.010

[13] He, Z. J., Xu, T., Song, B. D., & Tang, C. A. (2012). Numerical simulation study on the influence of FRP plate width on concrete interface bonding performance. *Building Structures*, (S1), 794–800. https://doi.org/10.19701/j.jzjg.2012.s1.196

[14] He, J. (2017). Research on the influence of adhesive properties on the interface bonding failure behavior of CFRP-solid materials [Doctoral dissertation]. Harbin Institute of Technology.

[15] Yang, Y., Huang, C. H., & Wu, Z. D. (2021). Research on the bonding performance of CFRP-steel plate interface based on double shear test. *Journal of Sun Yat-sen University (Natural Science Edition)*, (06), 62–70. https://doi.org/10.13471/j.cnki.acta.snus.2020.07.14.2020b082

[16] Wang, Z. Z., Zhou, Z., Bai, S., et al. (2020). Nonlinear analysis of the IC peel process of RC beams strengthened with end anchored CFRP plates. *Chinese Journal of Civil Engineering*, 53(1), 1–11.

[17] Lv, H. M., Peng, H., & Gong, S. (2025). Numerical study on the reinforcement of RC beams with additional non-prestressed section NSM CFRP. *Journal of Traffic Science and Engineering*, 41(02), 105–113. https://doi.org/10.16544/j.cnki.cn43-1494/u.20220316003

[18] Lv, H. M. (2022). Finite element analysis and experimental research on NSM CFRP strip reinforcement of concrete structures [Doctoral dissertation]. Changsha University of Science and Technology.

[19] Chen, L. L., Qiang, X. H., Xu, J., & Bai, J. (2024). Numerical study of steel–concrete composite beams strengthened by CFRP plates with prestressed unbonded reinforcement system. *Engineering Failure Analysis*, 157, 107905. https://doi.org/10.1016/j.engfailanal.2023.107905

[20] Lu, X. Z., Ye, L. P., Teng, J. G., & Jiang, J. J. (2005). Meso-scale finite element model for FRP sheets/plates bonded to concrete. *Engineering Structures*, 27(4), 564–575. https://doi.org/10.1016/j.engstruct.2004.10.010

[21] Lu, X. Z. (2004). Research on the interface behavior of FRP-concrete [Doctoral dissertation]. Tsinghua University.

ISSN: 2710-0588

[22] He, Z. J., Xu, T., Song, B. D., & Tang, C. A. (2012). Numerical simulation study on the influence of FRP plate width on concrete interface bonding performance. *Building Structures*, (S1), 794–800. https://doi.org/10.19701/j.jzjg.2012.s1.196

[23] Yang, Y., Huang, C. H., & Wu, Z. D. (2021). Research on the bonding performance of CFRP-steel plate interface based on double shear test. *Journal of Sun Yat-sen University (Natural Science Edition)*, (06), 62–70. https://doi.org/10.13471/j.cnki.acta.snus.2020.07.14.2020b082

[24] Li, T., Ning, Z. H., & Wu, J. Y. (2022). Experimental and numerical study on the bonding performance of CFRP reinforced steel plates in marine environment. *Materials Engineering*, 1–15.

[25] Yu, Q. Q., Zhao, Y. Z., & Gao, R. X. (2022). The influence of marine atmospheric environment on the interfacial bonding performance of CFRP-steel. *Composite Materials Science*, (11), 5148–5157. https://doi.org/10.13801/j.cnki.fhclxb.20220915.003

[26] Wu, H., Lu, S. F., & Chen, D. Research on the dynamic shear behavior of FRP-concrete bond interface based on 3D microscopic model of concrete. *Engineering Mechanics*, 1–16.

[27] Director, E., Ma, M. L., & Wang, Y. H. (2019). Analysis of reinforcement coefficient and parameters of prestressed CFRP plate bonded H-section steel beam. *Fiberglass Reinforced Plastics/Composites*, (04), 17–24.

[28] Wang, K. J. (2020). Numerical analysis of prestressed FRP reinforced concrete bending members [Master's thesis]. Dalian University of Technology. https://doi.org/10.26991/d.cnki.gdllu.2020.000428

[29] Lu, X. Z. (2004). Research on the interface behavior between FRP and concrete [Doctoral dissertation]. Tsinghua University.

[30] Feng, X. H. (2023). Experimental and simulation study on the bonding performance of CFRP-concrete interface under anchoring action [Doctoral dissertation]. Hebei University of Technology.